Hexagonal crystallization in a two-dimensional electron gas with disorder

Ulrich Wulf
Technische Universität Cottbus, Fakultät 1, Postfach 101344, 03013 Cottbus, Germany
(Received 6 June 1995)

We develop a theory for the solidification of the two-dimensional electron-gas in the presence of disorder. Our mean field theory includes the electron-electron interaction in the Hartree-Fock approximation and the potential of random impurities in the self-consistent Born approximation. It is shown that the electron solid is stable in a wide range of disorder strengths and that the impurity interaction leads to a considerable lowering of the ground-state energy. At low disorder we obtain a Wigner crystal with a gap in the density of states, and at stronger disorder a phase with a nonvanishing density of states is formed. In the presence of disorder there is still a sharp melting transition of the electron solid. Depending on the disorder strength it occurs at a significantly lower temperature. This can explain differences in recent experiments.

I. INTRODUCTION

There is strong experimental evidence for the solidification of a diluted electron gas, as predicted by Wigner,[1] on the surface of liquid helium[2] and in semiconductor heterostructures.[3] While in the first case the electrons are close to the classical limit, quantum fluctuations are important in the second system because of higher electron densities, a small band mass, and a relatively large dielectric constant of the semiconductor material. Therefore, in semiconductor heterostructures, an electron crystal only forms in the presence of a strong magnetic field helping to confine the electrons. A second important difference between the two systems is the presence of significant disorder in the heterostructures, which to a great extent stems from ionized impurities in the background.

Measurements on liquid helium[2] showed a ratio $\Gamma = e^2(\pi n)^{1/2}/k_B T_{\rm cl}^{B=0} = 137 \pm 15$ between the Coulomb energy of the classical electron lattice and the melting temperature $T_{\rm cl}^{B=0}$. In a theoretical analysis this was found to be consistent with a Kosterlitz-Thouless melting mechanism.[4,5] Experiments on the quantum crystal in the semiconductor system (Refs. 6–8) showed in the strong magnetic field limit a smaller melting temperature which decreases with increasing filling factor. Above a critical filling factor of about 0.22 there was no solid phase detected. Calculations assuming a Kosterlitz-Thouless type of dislocation mediated melting[9,10] are in fair agreement with these experiments. However, though the results of independent measurements—melting temperature versus filling factor—follow the same tendency, there is a systematic deviation[11] between them. For example, the melting temperatures by Andrei *et al.*[6] are consistently smaller by a factor close to 2 than the results of Goldman *et al.*[8] in the region of stable electron solid. To offer an explanation for these deviations and in view of the expected importance of the impurities in semiconductor heterostructures, we discuss a quantum theory of the stability of the Wigner crystal in the presence of disorder.

We find for low temperatures that the electron solid is stable in a wide range of disorder strengths and that the impurity interaction can lead to a considerable lowering of the ground-state energy. There are two types of solid phases: At weak disorder a crystal is formed with a gap in the density of states at the Fermi level, and at stronger disorder but still dominant Coulomb interaction another solid phase results with a nonvanishing density of states even in the zero-temperature limit. At a critical disorder strength there is a sharp transition to a disorder-dominated regime with a laterally homogeneous electron distribution. In the entire electron solid regime a sharp thermal melting transition occurs with decreasing melting temperature when the disorder increases. Though the absolute value of the melting temperature in mean-field theory is too high,[12] we note that the variation of the melting temperature in the electron solid regime is big enough to potentially account for the difference between the melting temperatures found in the measurements of Refs. 6–8.

II. FORMALISM

A. Model and general equations

We consider a Hamiltonian for the motion of the electrons containing three parts, the kinetic energy, the disorder potential of charged random impurities, and the electron-electron interaction. The disorder potential we take in the self-consistent Born approximation (SCBA). This approach has been succesfully used to describe impurity broadening of the Landau levels in the absence of the solidification of the electron gas.[13] As will be shown, this covers the limit of strong disorder. The electron-electron interaction we take in the Hartree-Fock approximation (HFA). As was demonstrated in Ref. 14, this approach gives very good results in the limit of vanishing disorder. Our model is thus able to interpolate between

0163-1829/95/52(16)/12120(6)/$06.00

the established results for vanishing and for strong disorder.

We treat as the undisturbed problem the Hamiltonian of the kinetic energy

$$H_0 = \frac{1}{2m}\left[\vec{p} + \frac{e}{c}\vec{A}\right]^2, \tag{1}$$

which describes the two-dimensional motion of a free electron in the x-y plane. The perpendicular magnetic field is taken in the Landau gauge, $\vec{A} = (0, Bx)$. As is well known, the eigenstates are then given by

$$\Psi_{N,X}(\vec{r}) = \left[2^N N!\sqrt{\pi} l L_y\right]^{-1/2} H_N\left(\frac{x-X}{l}\right) \times \exp\left[-\frac{(x-X)^2}{2l^2}\right] \exp\left[-i\frac{yX}{l^2}\right], \tag{2}$$

where $l = (eB/mc)^{1/2}$ is the magnetic length, H_N is a Hermite polynomial, and L_y is the length of the system in the y direction. The Landau-level index N determines the eigenenergies $\epsilon_N = \hbar\omega_c(N + 1/2)$ with the cyclotron frequency $\omega_c = eB/(mc)$. The condition $-L_x/2 < X < L_x/2$ and the periodic boundary conditions in the y direction, $X = m2\pi/L_y$ with integer m, lead to Landau levels with a degeneracy of $1/2\pi l^2$ neglecting spin. In the finite temperature Matsubara formalism the undisturbed Green's function is given by

$$G_0(\vec{r}, \vec{r'}, \omega_n) = \sum_{N,X} \frac{\Psi_{N,X}(\vec{r})\Psi^*_{N,X}(\vec{r'})}{i\hbar\omega_n - (\epsilon_N - \mu)}, \tag{3}$$

where $\omega_n = (2n+1)\pi/(\beta\hbar)$ are the fermionic Matsubara frequencies with $\beta = 1/(k_B T)$. To determine the Green's function we solve Dyson's equation,

$$G(\vec{r}, \vec{r'}, \omega_n) = G_0(\vec{r}, \vec{r'}, \omega_n) + \int d\vec{r''} d\vec{r'''} G_0(\vec{r}, \vec{r''}, \omega_n) \times \Sigma(\vec{r''}, \vec{r'''}, \omega_n) G(\vec{r'''}, \vec{r'}, \omega_n). \tag{4}$$

Evaluating standard diagrams in the finite temperature Matsubara formalism we obtain the self-energies of the impurity interaction in the SCBA and the Coulomb interaction in the HFA,

$$\Sigma(\vec{r}, \vec{r'}, \omega_n) = G(\vec{r}, \vec{r'}, \omega_n)\langle V_{\rm dis}(\vec{r}) V_{\rm dis}(\vec{r'})\rangle + \delta(\vec{r} - \vec{r'}) \int d\vec{r''} n(\vec{r''}) \frac{e^2}{|\vec{r''} - \vec{r'}|} - \frac{e^2}{|\vec{r} - \vec{r'}|} \frac{1}{\beta} \sum_{\omega_n} \lim_{\eta\to 0+} \exp(i\omega_n\eta) G(\vec{r}, \vec{r'}, \omega_n). \tag{5}$$

Here $\langle\,\rangle$ is the disorder average of the correlation function of the disorder potential $V_{\rm dis}(\vec{r})$. As usual the electron density is given by

$$n(\vec{r}) = \frac{1}{\beta} \lim_{\eta\to 0+} \sum_{\omega_n} \exp(i\omega_n\eta) G(\vec{r}, \vec{r}, \omega_n). \tag{6}$$

B. Method of solution

To solve Dyson's equation we use a representation

$$G(\vec{r}, \vec{r'}, z) = \sum_{N,X,X'} G_N(X, X', z) \Psi_{NX}(\vec{r}) \Psi^*_{NX'}(\vec{r'}) \tag{7}$$
$$= \sum_{N\vec{k}X} G_N(\vec{k}, z) \exp\left(ik_x X - i\frac{k_x k_y l^2}{2}\right) \times \Psi_{NX}(\vec{r}) \Psi^*_{N(X-k_y l^2)}(\vec{r'})$$

of the Green's function.[15] The Green's function is assumed diagonal in the Landau-level index. As a considerable numerical advantage $G_N(\vec{k}, z)$ depends only on one space argument, $\vec{k}$, which in addition is restricted to the hexagonal lattice. We choose the basis $\vec{k} = m\vec{k_1} + n\vec{k_2}$ with $\vec{k_1} = Q_0\vec{u}_y$ and $\vec{k_2} = Q_0/2(\sqrt{3}\vec{u}_x - \vec{u}_y)$, where $\vec{u}_{x/y}$ are the unit vectors in the Cartesian directions and $Q_0 = 4\pi/(\sqrt{3}a)$ with the nearest-neighbor distance a.

We begin to recast the general equations of the preceding subsection in the representation of Eq. (7) with the undisturbed Green's function for which we obtain

$$G^0_N(\vec{k}, z) = \delta_{\vec{k},0} \frac{1}{i\hbar\omega_n - (\epsilon_N - \mu)}. \tag{8}$$

Using Eq. (6) we obtain for the Fourier component $n(\vec{k}) = \int d^2\vec{r} \exp(-i\vec{k}\vec{r}) n(\vec{r})$ of the electron density

$$n(\vec{k}) = \frac{N_L}{\beta} \exp\left(\frac{-y^2}{4}\right) \sum_{\omega_n, N} L_N\left(\frac{y^2}{2}\right) \times \lim_{\eta\to 0+} \exp(i\omega_n\eta) G_N(-\vec{k}, \omega_n), \tag{9}$$

where $N_L = L_x L_y/(2\pi l^2)$ is the number of states in a Landau level, L_N is a Laguerre polynomial, and $y = |\vec{k}|l$. Performing a standard Matsubara frequency summation yields

$$n(\vec{k}) = N_L \exp\left(\frac{-y^2}{4}\right) \sum_N L_N\left(\frac{y^2}{2}\right) \rho_N(-\vec{k}), \tag{10}$$

where

$$\rho_N(\vec{k}) = -\frac{1}{\pi} \int_{-\epsilon}^{\epsilon} d\epsilon n_F(\epsilon) {\rm Im}\left[G_N(-\vec{k}, \epsilon - \mu + i\eta)\right], \tag{11}$$

with the Fermi distribution function $n_F(\epsilon) = \{\exp[(\epsilon - \mu)\beta] + 1\}^{-1}$. As usual the analytic continuation $i\omega_n \to z$ is made and the integration over ϵ is along the real axis where the imaginary part of the Green's function has a cut. The function $\rho_N(\vec{k})$ is the electron density projected onto the Nth Landau level in units of N_L. From Eqs. (10) and (11) we obtain the density of states

$$D(\epsilon) = -\frac{1}{\pi} \frac{1}{2\pi l^2} \sum_N {\rm Im}\left[G_N(\vec{k} = 0, \epsilon - \mu + i\eta)\right] \tag{12}$$

which is in agreement with Ando's results[13] without Coulomb interaction.

Inserting the transformation from Eq. (7) into Dyson's

equation yields

$$G_N(\vec{k},z) = G_N^0(\vec{k},z) + G_N^0(z)\sum_{\vec{p}} \Sigma_N(\vec{k}-\vec{p},z)G_N(\vec{p},z) \times \cos\left[\frac{l^2}{2}(\vec{k}\times\vec{p})_z\right]. \quad (13)$$

For the self-energy we obtain a representation $\Sigma_N(\vec{k},z)$ like for the Green's function, with $\Sigma_N(\vec{k},z) = \Sigma(\vec{k},z)_N^{\rm dis} + \Sigma(\vec{k},z)_N^{\rm HF}$. We note that Eq. (13) has the form of a simple matrix equation in the space of the reciprocal lattice vectors and can thus be solved with standard numerical techniques. In practice the Green's function has to be evaluated only along the real axis of the complex z plane. For the self-energy of the impurity interaction we can directly adopt the general results of Ref. 15. There it has been shown that we can write for an ensemble of δ scatterers with individual scattering potentials of $v(r) = V_0\delta(r)$

$$\Sigma_N^{\rm dis}(\vec{k},z) = \frac{1}{4}G_N(\vec{k},z)\Gamma_N^2(\vec{k}), \quad (14)$$

with

$$\Gamma_N^2(\vec{K}) = \Gamma^2 L_N^2\left(\frac{y^2}{2}\right)\exp\left(-\frac{y^2}{2}\right), \quad (15)$$

where $\Gamma = 4n_I V_0^2/2\pi l^2$ and n_I is the number of scatterers per area. For the self-energy of the Hartree-Fock term it follows that

$$\Sigma(\vec{k},z)_N^{\rm HF} = W_N(\vec{k})\rho_N(\vec{k}) \quad (16)$$

with

$$W_N(\vec{k}) = \frac{e^2}{l}\left[\int_0^\infty du \exp\left(-\frac{u^2}{2}\right)L_N^2\left(\frac{u^2}{2}\right)J_0(uy) + \frac{1}{y}\exp\left(-\frac{y^2}{2}\right)L_N^2\left(\frac{y^2}{2}\right)(1-\delta_{\vec{k},0})\right]. \quad (17)$$

Here the first factor comes from the Fock term and the second factor contains the contribution of the Hartree term as well as the interaction with a homogeneous positive background. In this paper we consider the case in which only the lowest Landau level is occupied. Then we can restrict ourselves to the solution of Dyson's equation for only the lowest Landau level for which we have[16]

$$W_0(\vec{k}) = \frac{e^2}{l}\exp\left(-\frac{y^2}{2}\right)\left[\frac{1}{y}(1-\delta_{\vec{k},0}) - \left(\frac{\pi}{2}\right)^{1/2} I_0\left(\frac{y^2}{4}\right)\right]. \quad (18)$$

Here I_0 is the modified Bessel function of the first kind.

C. Ground-state energy

To determine the ground-state energy from the solution of Eq. (7) we start from the general expression for interacting fermions,[17]

$$E_0 = \frac{1}{2\beta}\int d\vec{r}\lim_{\vec{r}'\to\vec{r}}\sum_n \exp(i\omega_n\eta)\left[i\hbar\omega_n - \frac{1}{2m}\left(\vec{p}+\frac{e}{c}\vec{A}\right)^2 + U(\vec{r}) + \mu\right]G(\vec{r},\vec{r}',\omega_n), \quad (19)$$

where $U(\vec{r})$ is the single particle potential of the random impurities and the spin degree of freedom has been neglected. Making use of the relation

$$\left[i\hbar\omega_n + \frac{1}{2m}\left(\vec{p}+\frac{e}{c}\vec{A}\right)^2 - U(\vec{r}) + \mu\right]G(\vec{r},\vec{r}',\omega_n) = \delta(\vec{r}-\vec{r}') + \int d\vec{r}_2\Sigma_{\rm HF}(\vec{r},\vec{r}_2)G(\vec{r}_2,\vec{r}',\omega_n) \quad (20)$$

valid in the Hartree-Fock approximation, we can express the ground-state energy in terms of the self-energy and the Green functions for which we use the numerical results from the solution of the Dyson equation [Eq. (13)]. After further manipulation we obtain

$$\epsilon_0 = \frac{1}{\nu}\int dE n_F(E)D(E)E - \frac{1}{2\nu}\sum_{\vec{k}} W_0(\vec{k})\langle\rho(-\vec{k})\rangle\langle\rho(\vec{k})\rangle. \quad (21)$$

Here ϵ_0 is the ground-state energy per particle.

III. RESULTS

A. Density of states

The changes in the ground state of the system in dependence of the impurity strength are illustrated in Fig. 1. We plot the density of states in the two-dimensional electron system at varying disorder strengths. In the limit of strong impurity interaction the formation of a charge density wave is suppressed and we obtain an average density distribution that is laterally homogeneous. In this limit the results of Ando[13] for the density of states of an electron gas without Coulomb interaction are recovered. A trivial shift of the energy zero to lower values is

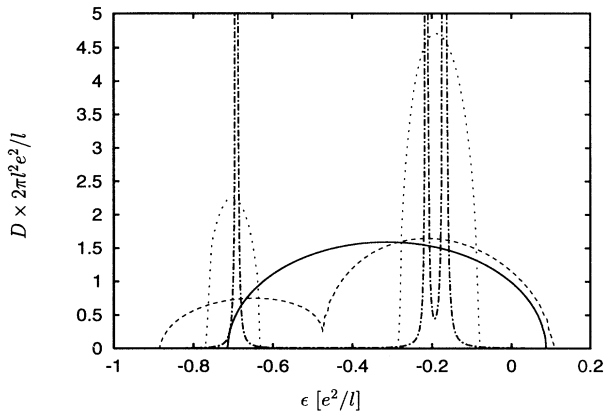

FIG. 1. Density of states vs energy for $\nu = 1/4$ and $\beta = 0.02e^2/l$. Solid line, $\Gamma = 0.4e^2/l$; dashed line, $\Gamma = 0.34e^2/l$; and dotted line, $\Gamma = 0.1e^2/l$. The dash-dotted line is the result of a calculation taking into account impurity broadening only by a very small Lorentz line broadening of $\delta = 10^{-3}e^2/l$. At smaller δ the highest subband splits into two bands leading to a total of four energy bands.

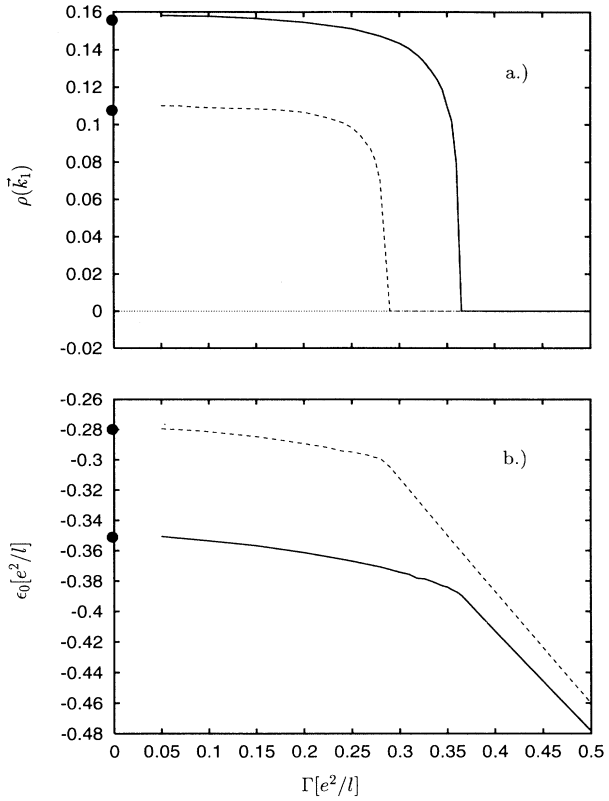

FIG. 2. (a) The order parameter $\rho(\vec{k}_1)$ at $\beta = 0.02e^2/l$. Solid lines, $\nu = 1/4$; dashed lines, $\nu = 1/7$. The circles at $\Gamma = 0$ represent the result of Eq. (22). (b) Ground-state energy per particle, line code like in (a). Here the full circles are the result of Eq. (23).

caused by the $\vec{q} = 0$ term of the Fock term in the Coulomb interaction [Eq. (18)]. With decreasing disorder a local minimum of the density of states at the Fermi energy develops and turns into an energy gap separating occupied and unoccupied states. This energy gap reflects the formation of an insulating Wigner crystal. With further decreasing disorder the energy bands become narrower without a significant shift of the positions of their center and the energy gap widens. At very small disorder the upper band splits in three subbands yielding a total of four energy bands to be expected at $\nu = 1/4$.[15]

B. Disorder melting of the Wigner crystal

To gain a more quantitative insight into how the Wigner crystal interacts with the impurity potential we plot as an order parameter the Fourier component of the electron density belonging to one first-shell lattice vector of the reciprocal lattice [Fig. 2(a)]. Because of long-wavelength fluctuations, either of thermal origin[18] or in the impurity potential,[19] we cannot expect true long-range order. We thus interpret the order parameter as describing domains of short-range order in the disordered system. From our results, we can distinguish two regions: For weak disorder, in the electron solid regime, the order parameter is well approximated by the strong-magnetic-field limit[16]

$$\rho(\vec{k}_1) = \nu \exp\left(-|\vec{k}_1 l|^2/4\right). \tag{22}$$

There is only a weak dependence of the order parameter on the impurity potential. At stronger disorder there is an abrupt transition to the regime of dominant disorder where the order parameter vanishes. It occurs at a value of Γ that is close to the correlation energy $\epsilon_{\mathrm{WC}}^{\mathrm{HF}}$ of the Wigner crystal (WC) without impurities. Using the interpolation formula

$$\epsilon_{\mathrm{WC}}^{\mathrm{HF}}[e^2/l] = -0.782\,133\nu^{1/2} + 0.2823\nu^{3/2} + 0.18\nu^{5/2} - 1.41\exp\left(-2.07/\nu\right) \tag{23}$$

from Ref. 14 we obtain for $\nu = 1/4$, $\epsilon_{\mathrm{WC}}^{\mathrm{HF}} = -0.3505$ and for $\nu = 1/7$, $\epsilon_{\mathrm{WC}}^{\mathrm{HF}} = -0.2794$. Figure 2(b) shows the ground-state energy as a function of the impurity strength. At both filling factors there is a discontinuity in the derivative of the energy with respect to Γ where the order parameter goes to zero. This discontinuity and the jump in the order parameter we interpret as a crossover from a system with a short-range electron solid order to a system with completely suppressed charge density wave order. This crossover can well be identified as a phase transition experimentally.

In addition to the discontinuity of the derivative with respect to Γ there is a small dip in the ground-state energy which occurs at $\Gamma \approx 0.24e^2/l$ for $\nu = 1/7$ and $\Gamma \approx 0.32e^2/l$ for $\nu = 1/4$. It turns out that above these values of Γ the energy gap is zero and below these values the width of the gap increases with decreasing disorder. Therefore there is a range of disorder strength, for

$\nu = 1/4$ it is $0.32e^2/l < \Gamma < 0.35e^2/l$, in which there is no gap in the density of states but a considerable lateral modulation of the electron density. It can be expected that the absence of an energy gap has a qualitative impact on the transport properties of the electron solid.

We note that the energy decrease of the electron solid due to the interaction with the impurities can be in the order of about 5% of the correlation energy. For example, at $\nu = 1/7$ we obtain $[\epsilon_0(\Gamma = 0.25) - \epsilon_0(\Gamma = 0.05)]/\epsilon_0(\Gamma = 0.05) = 5.6 \times 10^{-2}$. This is conceivable compared to the difference in the ground-state energies of the correlated Wigner crystal ϵ^c_{WC} without disorder and the Laughlin liquid ϵ_L. For $\nu = 1/7$ we compare $\epsilon_L = -0.2810e^2/l$ of Ref. 20 with $\epsilon^c_{WC} = -0.2816e^2/l$ (Ref. 14) and obtain $(\epsilon^c_{WC} - \epsilon_L)/\epsilon^c_{WC} = 2.1 \times 10^{-3}$.

C. Thermal melting of the disordered Wigner crystal

In Fig. 3 we show the temperature dependence of the order parameter at different values of disorder strength. In all cases there is a rather sharp transition at which the order parameter goes to zero allowing us to define a melting temperature. With increasing Γ the melting temperature T_m decreases strongly (see also Fig. 4). For example, at $\nu = 1/4$ we obtain at $\Gamma = 0.355e^2/l$ a melting temperature of about $0.02e^2/l$ which is about a factor 5 smaller than $T_m = 0.11e^2/l$ at low disorder ($\Gamma = 0.1e^2/l$). Our melting temperatures in the low disorder limit are in agreement with the results of Refs. 21–23 which can well be approximated by

$$k_B T_m = 0.557\nu(1-\nu)e^2/l. \qquad (24)$$

From Eq. (24) we obtain $k_B T_m = 0.1044e^2/l$ for $\nu = 1/4$ and $k_B T_m = 0.068e^2/l$ for $\nu = 1/7$. Though the absolute temperature of the melting transition is too big in mean-field theory its variation with varying disorder strength can account for the deviations by a factor of about 2 in the independent measurements.[11]

We distinguish two different domains: At small disorder ($\Gamma = 0.1$, 0.2) the order parameter is nearly constant

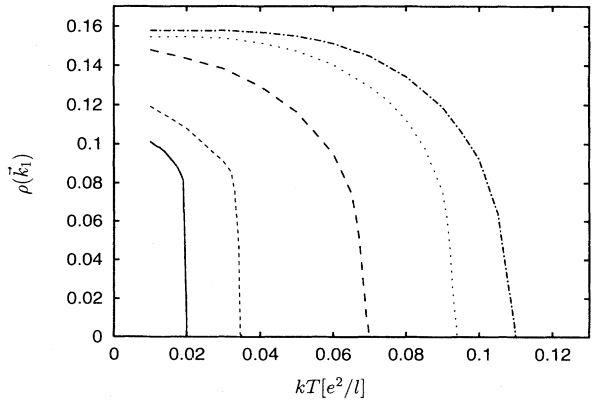

FIG. 3. Temperature dependence of the order parameter for $\nu = 1/4$. Solid line, $\Gamma = 0.36e^2/l$; short-dashed line, $\Gamma = 0.35e^2/l$; long-dashed line, $\Gamma = 0.3e^2/l$; dotted line, $\Gamma = 0.2e^2/l$; and dash-dotted line, $\Gamma = 0.1e^2/l$.

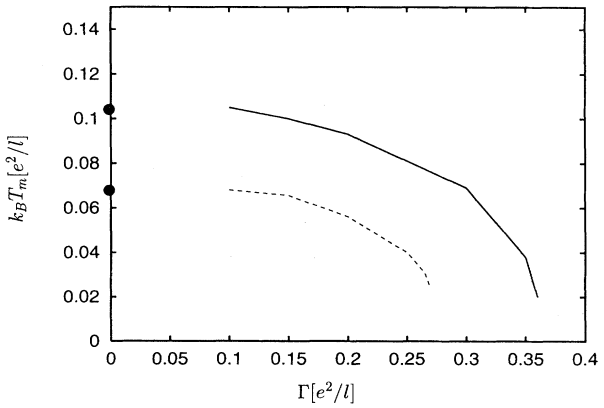

FIG. 4. Melting temperature vs impurity strength Γ for $\nu = 1/4$ (solid line) and $\nu = 1/7$ (dashed line). The full circles mark the results of the approximation in Eq. (24).

at low temperatures (below about $0.02e^2/l$) whereas when the impurity potential is stronger ($\Gamma = 0.36$, $\Gamma = 0.35$) the order parameter grows continually with decreasing temperature in the range of numerically accessible temperatures. Also, at strong disorder the order parameter vanishes more abruptly with increasing temperatures when the crystal melts. That these are two

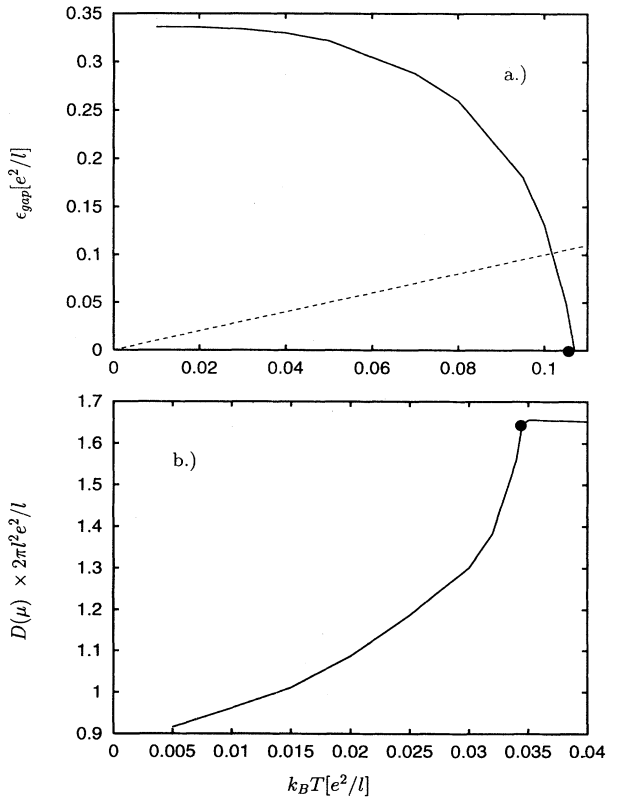

FIG. 5. (a) Width of the energy gap vs temperature at $\Gamma = 0.1$ and $\nu = 1/4$; dashed line, thermal energy $k_B T$. (b) Density of states at the Fermi energy vs temperature for $\Gamma = 0.35$ and $\nu = 1/4$. The full circles mark the position at which the jump in $\rho(\vec{k}_1)$ takes place.

qualitatively different domains is demonstrated in Fig. 5. At small disorder there is an energy gap at the Fermi level when the charge density wave is formed. This energy gap can be associated with a crystalline phase. At small temperatures the thermal energy is much smaller than the width of the gap and the order parameter, thus becomes independent of the temperature. With increasing temperature the gap becomes smaller and the crystal melts when it becomes smaller than the thermal energy. At strong disorder even in the limit of zero temperature there is no energy gap. Though there is a nonzero order parameter, the density of states at the Fermi level remains finite. This is consistent with the formation of a phase in which due to the impurity interaction the electrons are not rigidly pinned to their position in the hexagonal lattice. A significant hopping transport therefore should be possible. However, the dominant Coulomb interaction is expected to influence the hopping transport strongly,[24] which will be analyzed in a later study.

In conclusion we present a theory of the Wigner crystal in disorder. Our results show that the electron solid is stable in a wide range of impurity strengths and that the ground-state energy can be lowered significantly in the disorder potential. Also, we obtain a pronounced decrease of the melting temperature in the presence of disorder. This can explain the deviations in the experimental melting curves of different experiments.[11] At strong disorder not a Wigner crystal but a phase with a nonvanishing density of states at the Fermi level is formed.

ACKNOWLEDGMENT

The author thanks A. H. MacDonald for valuable discussions.

[1] E. P. Wigner, Phys. Rev. **46**, 1002 (1934).
[2] C. C. Grimes and G. Adams, Phys. Rev. Lett. **42**, 795 (1979).
[3] H. W. Jiang, R. L. Willet, H. L. Stormer, D. C. Tsui, L. N. Pfeiffer, and K. W. West, Phys. Rev. Lett. **65**, 633 (1990); V. M. Pudalov and S. T. Chui, Phys. Rev. B **49**, 14 062 (1994); H. Buhmann, W. Joss, K. v. Klitzing, I. V. Kukushkin, A. S. Plaut, G. Martinez, K. Ploog, and V. B. Timofeev, Phys. Rev. Lett. **66**, 926 (1991); A. A. Shashkin, V. T. Dolgopolov, G. V. Kravchenko, M. Wendel, R. Schuster, J. P. Kotthaus, R. J. Haug, K. v. Klitzing, K. Ploog, H. Nickel, and W. Schlapp, *ibid.* **73**, 3141 (1994); I. V. Kukushkin, V. I. Fal'ko, R. J. Haug, K. v. Klitzing, K. Ebert, and K. Tötemayer, *ibid.* **72**, 3594 (1994).
[4] D. J. Thouless, J. Phys. C **11**, 1189 (1978).
[5] R. H. Morf, Phys. Rev. Lett. **43**, 931 (1979).
[6] E. Y. Andrei, G. Deville, D. C. Glattli, and F. I. B. Williams, Phys. Rev. Lett. **60**, 2765 (1988).
[7] R. L. Willet, H. L. Stormer, D. C. Tsui, L. N. Pfeiffer, and K. W. West, Phys. Rev. B **38**, 7881 (1988).
[8] V. J. Goldman, M. Santos, M. Shayegan, and J. E. Cunningham, Phys. Rev. Lett. **65**, 2189 (1990).
[9] S. T. Chui and K. Esfarjani, Europhys. Lett. **14**, 361 (1991).
[10] S. T. Chui and K. Esfarjani, Phys. Rev. B **44**, 11 498 (1991).
[11] A good summary of the experimental results is in Ref. 10, Fig. 2.
[12] K. Maki and X. Zotos, Phys. Rev. B **28**, 4349 (1983).
[13] T. Ando, A. B. Fowler, and F. Stern, Rev. Mod. Phys. **54**, 437 (1982).
[14] P. K. Lam and S. M. Girvin, Phys. Rev. B **30**, 474 (1984).
[15] U. Wulf and A. H. MacDonald, Phys. Rev. B **47**, 6566 (1993).
[16] R. Cote and A. H. MacDonald, Phys. Rev. B **44**, 8759 (1991); Surf. Sci. **263**, 187 (1992); Phys. Rev. Lett. **65**, 2662 (1990).
[17] A. Fetter and J. Walecka, in *Quantum Theory of Many-Particle Systems* (McGraw-Hill, San Francisco, 1971), Chap. 8.
[18] N. D. Mermin, Phys. Rev. **176**, B250 (1968).
[19] U. Wulf, V. Gudmundsson, and R. R. Gerhardts, Phys. Rev. B **38**, 4218 (1988).
[20] D. Levesque, J. J. Weis, and A. H. MacDonald, Phys. Rev. B **30**, 1056 (1984).
[21] H. Fukuyama, P. M. Platzmann, and P. W. Anderson, Phys. Rev. B **19**, 5211 (1979).
[22] R. R. Gerhardts, Phys. Rev. B **24**, 1339 (1981).
[23] R. R. Gerhardts and Y. Kuramoto, Z. Phys. B **44**, 301 (1981).
[24] H. Böttger and V. V. Bryksin, *Hopping Conduction in Solids* (VCH Verlagsgesellschaft, Weinheim, 1985).